The Journal of Experimental Biology 207, 3035-3042
Published by The Company of Biologists 2004
doi:10.1242/jeb.01122

Experimental studies of the material properties of the forewing of cicada (Homóptera, Cicàdidae)

F. Song[1], K. L. Lee[2], A. K. Soh[2,*], F. Zhu[2] and Y. L. Bai[1]

[1]*State Key Laboratory of Nonlinear Mechanics (LNM), Institute of Mechanics, Chinese Academy of Sciences, Beijing 100080, People's Republic of China* and [2]*Department of Mechanical Engineering, The University of Hong Kong, Hong Kong, People's Republic of China*

*Author for correspondence (e-mail: aksoh@hkucc.hku.hk)

Accepted 2 June 2004

Summary

Detailed investigations on the structural and mechanical properties of the forewing of the cicada were carried out. Measurement of the structures of the wings showed that the thickness of the membrane of each cell and the diameter of each vein were non-uniform in both the longitudinal and transverse directions, and their means were approximately 12.2 and 133.3 μm, respectively. However, the aspect ratios of the wings and the bodies were quite uniform and were approximately equal to 2.98 and 2.13, respectively. Based on the measured thickness, mass and area of the membranes of the cells, the mean density and the mean area density of the wing were approximately 2.3 g cm^{-3} and 2.8×10^{-3} g cm^{-2}, respectively. In addition, the diameters of the veins of the wings, including the diameters of the holes in the vein of the leading edge, were examined. The mechanical properties of the wing were investigated separately by nanoindentation and tensile testing. The results indicated that the mean Young's modulus, hardness and yield stress of the membranes of the wings were approximately 3.7 GPa, 0.2 GPa and 29 MPa, respectively, and the mean Young's modulus and strength of the veins along the direction of the venation of wings were approximately 1.9 GPa and 52 MPa, respectively. Finally, the relevant results were briefly analyzed and discussed, providing a guideline to the biomimetic design of the aerofoil materials of micro air vehicles.

Key words: cicada, Homoptera, wing, membrane, vein.

Introduction

The material properties of the wings of insects are determined primarily by the need to optimize the production of favorable aerodynamic forces during flight (Wootton, 1992; Chapman, 1998). Flight, however, is not a simple matter of flapping the wings up and down. In addition, the wings are brought forward and backward and twisted; that is, either the leading edge is turned downward or the trailing edge is turned backward. These wing movements apparently involve some complex mechanical and aerodynamic performances of the wings (Borror et al., 1989).

The fully developed wings of all insects normally consist of two components: membrane and vein. From the mechanical viewpoint, the form of an individual vein reflects its role in the production of useful aerodynamic forces by the wing as a whole. Especially on the leading edge of the wing, the longitudinal veins form a rigid span supporting the wing as it moves through the air (Wootton, 1992). The structural and mechanical properties of the wing are obviously intimately associated with the flight capacity of insects. However, to date, the aerodynamically relevant material properties of wings themselves have hardly been studied in detail, with the exception of Wootton's group, who have specifically studied the structural and mechanical properties of the hindwings of locusts (Jensen and Weis-Fogh, 1962; Banerjee, 1988; Wootton et al., 2000; Smith et al., 2000; Herbert et al., 2000), whereas the dynamic mechanisms of the flight of insects have been widely investigated recently (Ellington et al., 1996; Van Den Berg and Ellington, 1997; Dickinson et al., 1999; Birch and Dickinson, 2001; Weis-Fogh and Jensen, 1956; Maxworthy, 1979).

The wings of insects have very complex structures. Their mechanical responses to applied loads are due partly to gross structure and partly to the properties of the materials from which these components are constructed (Smith et al., 2000). In terms of the morphological and mechanical properties of the wing membrane of the insects during flight, Wootton et al. (2000) pointed out that the membrane is not simply a barrier to the passage of air through the wing but, in some areas at least, has a structural role as a stressed skin, stiffening the framework of veins. And there may be local variation in the mechanical properties and, hence, in the structure of the membrane within the wing, with profound implications for its functioning in flight. Therefore, both gross structure and material properties need to be taken into account in any rigorous engineering analysis.

More recently, for the sake of biomimetic design of the aerofoil of micro air vehicles, the flight of cicadas has become an attractive research topic (Ho et al., 2002; Fearing et al., 2000), even though the cicada is actually famous for its song (Fonseca et al., 2000; Fonseca and Revez, 2002). Such research interest is attributed to the fact that (1) although the weight of the body of the cicada is almost 100 times more than that of its own wings, these wings are still able to lift the heavy body in the air with no difficulty and fly rapidly and agilely and (2) the wing structure of the cicada, in particular the arrangements of the venation of the wings, is much simpler than that of other insects with a big and heavy body, such as locusts or dragonflies, and therefore such wings can be easily mimicked in the design of aerofoil of small vehicles. However, to date, the material properties of the wings of the cicada have never been systematically investigated. Note that even the study of the structural and mechanical properties of the wings of the cicada, from the viewpoint of biology, is of considerable merit.

Traditionally, measurements of the properties of the wings of insects mainly use the methods of tensile testing by some mechanical-test machines (Smith et al., 2000). However, tensile testing is very difficult for some small-scale samples of insect's wings, such as when measuring the mechanical properties of a cell (a compartment of membrane between wing veins). Therefore, it is necessary to find a testing method that can more conveniently and accurately measure the mechanical properties of small-scale samples, such as the cells of insects.

The nanoindentation technique is an excellent tool for the study of the mechanical behavior of thin membranes, in particular when simple tensile tests are difficult to perform. The development of the nanoindentation technique has allowed highly localized hardness and modulus measurements to be performed on very small material volumes. In principle, if a very sharp tip is used, the contact area between the sample and the tip, and thus the volume of material that is tested, can be made arbitrarily small. Usually, the indented area is difficult to measure by microscope. Thus, the load and displacement during the indentation process are recorded and these data are analyzed to obtain the contact area and mechanical properties.

In the present study, our investigations focus on the structural and mechanical properties of the forewings of the cicada, in particular the membranes and veins of the wings. By means of some experimental techniques, we obtained the relevant geometrical and physical characteristics of the wings. Based on these characteristics, the Young's modulus and the strength of the membranes and veins of the wings were measured using the methods of nanoindentation and tensile testing, respectively. The results obtained by these two testing methods are in good agreement. Finally, we briefly analyzed and discussed all the results.

Materials and methods

Preparation

All test samples of the wings were taken from cicadas (*Magicicàda*) that were caught on the mountain near the University of Hong Kong. For testing of both the structural and the mechanical properties of the wings, the wing samples were first washed using distilled water and then air-dried at room temperature (20–25°C). This preparation was carried out in the laboratory within 48 h after the cicadas had been caught.

Based on the fact that the wing material properties change fairly rapidly after being removed from the insect (Smith et al., 2000), all mechanical testing samples were directly removed from the relevant region of the forewings of living cicadas and rapidly installed and examined on the relevant experimental machines within ~10 min. Therefore, the examined properties of the materials are deemed approximately the same as those of the parts of a living cicada.

Structural measurements

The morphological and geometrical characteristics of the forewings of cicadas were determined as follows. The length and width of the wings and the bodies were measured using an electronic caliper with ±0.1 mm accuracy (Mitutoyo, Takatsu-ku, Kawasaki, Japan), and the mass of the wings and bodies was measured using an electronic balance with ±0.1 mg accuracy (Mitutoyo). The thickness of the membrane cells and the diameter of the veins of the wings were measured using a micrometer gauge with ±0.1 μm accuracy (Mitutoyo).

In order to measure the real area of the wing, we used a rectangle, which had the area of span × chord of the wing being measured and was equally divided into 100×100 grids, to cover the pictures of the wings measured on the computer. We then removed any grids that did not cover any parts of the wings. The remaining number of grids was considered to be the approximate area of the wings.

Mechanical testing

In order to measure the mechanical properties of the forewings of the cicada, indentation experiments were first carried out using a nanoindenter (TriboScope, Hysitron INC, Minneapolis, MN, USA) with a Berkovich diamond indenter tip (TriboScope) to test the membrane of each and every cell on the wings.

The membrane of each cell was cut off from the wings to be tested and separately glued on a substrate material using instant adhesive (3M, No. 171). Pure Nickel circular plates, whose hardness, diameter and thickness were 0.26 GPa, 20 mm and 2 mm, respectively, were used as substrates. In order to determine the modulus of the membrane accurately using the nanoindentation technique, the adhesive between the membrane and the plate should, firstly, be paved as thin and uniform as possible and, secondly, the line profile of the membrane surface should be measured by the nanoindenter.

Based on the theory of nanoindentation, the reduced modulus, E_r, can be evaluated from the nanoindentation measurements by employing the following equation:

$$E_r = \frac{\sqrt{\pi}(\mathrm{d}P/\mathrm{d}h)_{\mathrm{unload}}}{2\sqrt{A(h_c)}}, \quad (1)$$

where P is the indentation load; h and h_c are the penetration and contact depths, respectively, and A is the contact area, which is a function of the contact depth. The contact depth at the maximum load is given by:

$$h_c = h_{max} - 0.75\,\frac{P_{max}}{S}\,, \tag{2}$$

where S=dP/dh at h=h_{max}, and 0.75 is a constant that depends on the indenter geometry.

For evaluating E_r, the contact stiffness, $(dP/dh)_{unload}$, and the contact area A should be determined accurately from load against displacement graph measured during the indentation process. The least mean squares method was employed for fitting to 90% of the unloading curve according to the hypothesis that the unloading data can be expressed as a power law (Oliver and Pharr, 1992):

$$P = A(h - h_f)^m\,, \tag{3}$$

where A and m are empirically determined fitting parameters, and h_f is the final penetration depth. Fig. 1A shows a schematic sketch of the Oliver and Pharr model with the definition of h_f, h_c, h_i and h_{max}, while Fig. 1B shows the schematic representation of the indentation process.

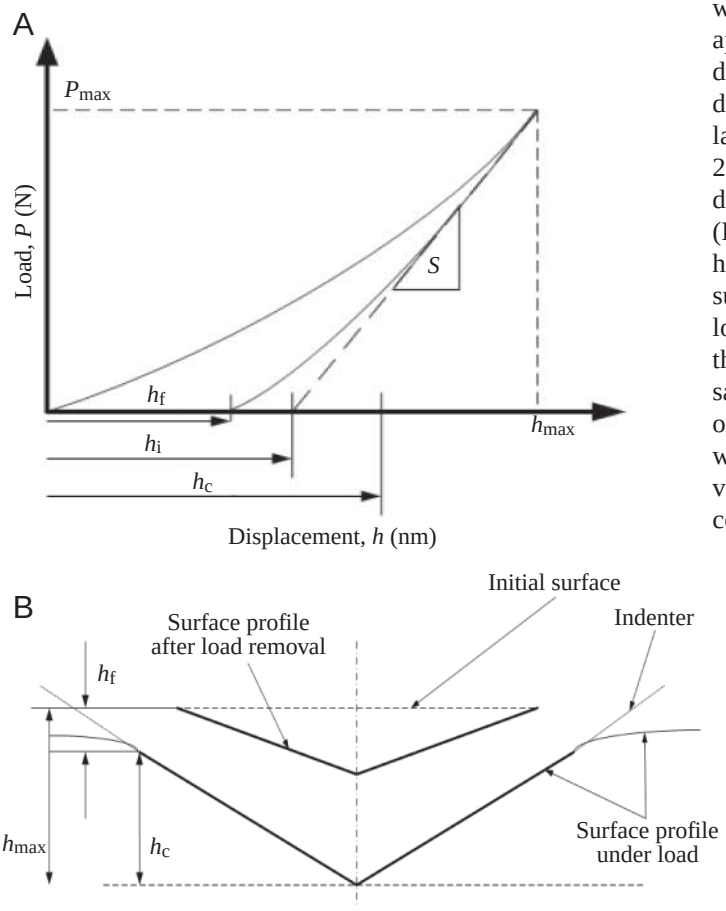

Fig. 1. (A) Schematic plot of the Oliver and Pharr (1992) model. (B) Schematic representation of the indentation process, in which S is dP/dh (see equation 2), h_c is the contact depth, h_f is the final penetration depth, h is the penetration depth and h_{max} is maximum penetration depth.

The expression for the contact area using the Berkovich indenter is approximated by the following formula:

$$A = 24.5h_c^2\,. \tag{4}$$

The hardness (H) can be obtained from the following equation:

$$H = \frac{P_{max}}{A}\,. \tag{5}$$

The effects of a non-rigid indenter on the load displacement behavior can be taken into account by defining an effective modulus, E_r, as follows:

$$\frac{1}{E_r} = \frac{1-\nu^2}{E} + \frac{1-\nu_i^2}{E_i}\,, \tag{6}$$

where E is Young's modulus and ν is Poisson's ratio of the specimen; E_i and ν_i are the corresponding values of the indenter. For the diamond indenter used in our experiments, E_i=1141 GPa and ν_i=0.07. Also, in all calculations, ν is assumed to be 0.25. From equations 1–6, Young's modulus and the hardness of the membrane can be obtained.

The hardness and elastic modulus of the membrane were measured by employing the multi-cycles testing method, in which a sequence of multiple loading–unloading cycles was applied at the same lateral position. This method enables the determination of material properties with varying indentation depth. Moreover, the data collected are not affected by the lateral lack of homogeneity of the sample (Wolf and Richter, 2003). This is important since the membrane cannot be deposited to the substrate using physical vapor deposition (PVD) or chemical vapor deposition (CVD), which ensures homogeneity of the adhesive between the membrane and the substrate system. Note that for each cycle, the indenter was loaded to a certain prescribed load over 5 s and then held at this peak load for 10 s prior to being unloaded to 10% of the said peak load. A sequence of 10 loading–unloading cycles in one experiment was performed. Five to seven indentations were made on each membrane cell in order to obtain the mean values. The nanoindentation load, together with the corresponding displacement data, was analyzed by employing the method of Oliver and Pharr (1992) to determine the nanoindentation hardness and elastic modulus. However, it is difficult to examine the modulus of the vein using the nanoindentation method, since the center of the vein of the wing is hollow in shape.

Secondly, the mechanical properties of the wings, including the membranes and the veins, were measured using the material-testing instrument (LLOYD, LR 5K, Fareham, UK). In the testing process, we controlled the extensive displacement of each of the testing samples by the instrument at a loading rate of 0.5 mm min^{-1} until the testing sample was ruptured. Simultaneously, the applied tensile loads can be automatically recorded by the material-testing instrument.

Some samples were prepared by cutting the veins from the leading edges of the wings. The width and length of

each of the vein samples tested were approximately 1.75 and 30 mm, respectively, and the thickness of the samples was the same as the diameter of a vein at the leading edges. Note that the testing span of each of the samples was 20 mm. Similarly, each of the membrane samples used for tensile testing was cut off from the cells of the wings. The width and length of each of the membrane samples, which were without any vein, were approximately 2 and 15–20 mm, respectively; the thickness of the samples was the same as that of the cell. Note that the testing span of each of the membrane samples was 10 mm.

According to the principle of the tensile testing of materials, the material strain can be taken as:

$$\varepsilon = \Delta l/l_0 , \quad (7)$$

where Δl is the increase of length in the tensile direction of the material, and l_0 is the original testing span of the sample. Correspondingly, the material stress can be calculated as follows:

$$\sigma = F/A_0 , \quad (8)$$

where F is the tensile force applied on the specimen, and A_0 is the original cross-sectional area of the specimen. In equations 7 and 8, l_0 and A_0 were determined using the structural data of the wings given above; Δl and F can be obtained by tensile testing of the materials. By employing Hooke's law, the Young's modulus of the material is given by:

$$E = \sigma/\varepsilon . \quad (9)$$

From equations 7–9, Young's modulus of the materials can be obtained. However, in order to accurately determine the Young's modulus, the force and deformation should correspond to the linear elastic part of the experimental curve of the samples measured. Due to the non-linear characteristics of biomaterials, the elastic force and deformation do not exhibit a clearly defined elastic limit. Thus, in the present study, we employ a common practice of using the offset method. The amount of 0.02% is set off on the strain or extension axis, and a line is drawn parallel to the straight line portion of the loading curve; the intersection point gives the stress of the elastic limit. Therefore, the slope calculated is deemed the Young's modulus of the biomaterials.

Results

Morphological tests

Fig. 2A shows the forewing and body of the cicada and the relevant definitions. The relevant measured results, which were taken from five cicadas, are shown in Table 1, in which A represents the area of the wing, which was approximated as $0.72bc$, by employing the computer grid method to estimate the wing area as stated above, M_b and M_w denote the mass of the body and wing, respectively, and σ denotes the area density of the wing. Note that since the right and left forewings of some samples were not necessarily identical, the data presented in Table 1 were the average values.

From Table 1, the aspect ratio of the forewings, b/c, is calculated as ~2.98±0.05 (mean ± S.D.), while that of the bodies, L/W, is ~2.13±0.02 (mean ± S.D.). In terms of the samples we studied here, it was interesting to note that the aspect ratios of both the forewings and bodies of cicadas were more or less constant. In addition, it can be seen from the same table that the area densities (σ) of the wings tested were all about the same, and the mean value is 2.8×10^{-3} g cm^{-2}.

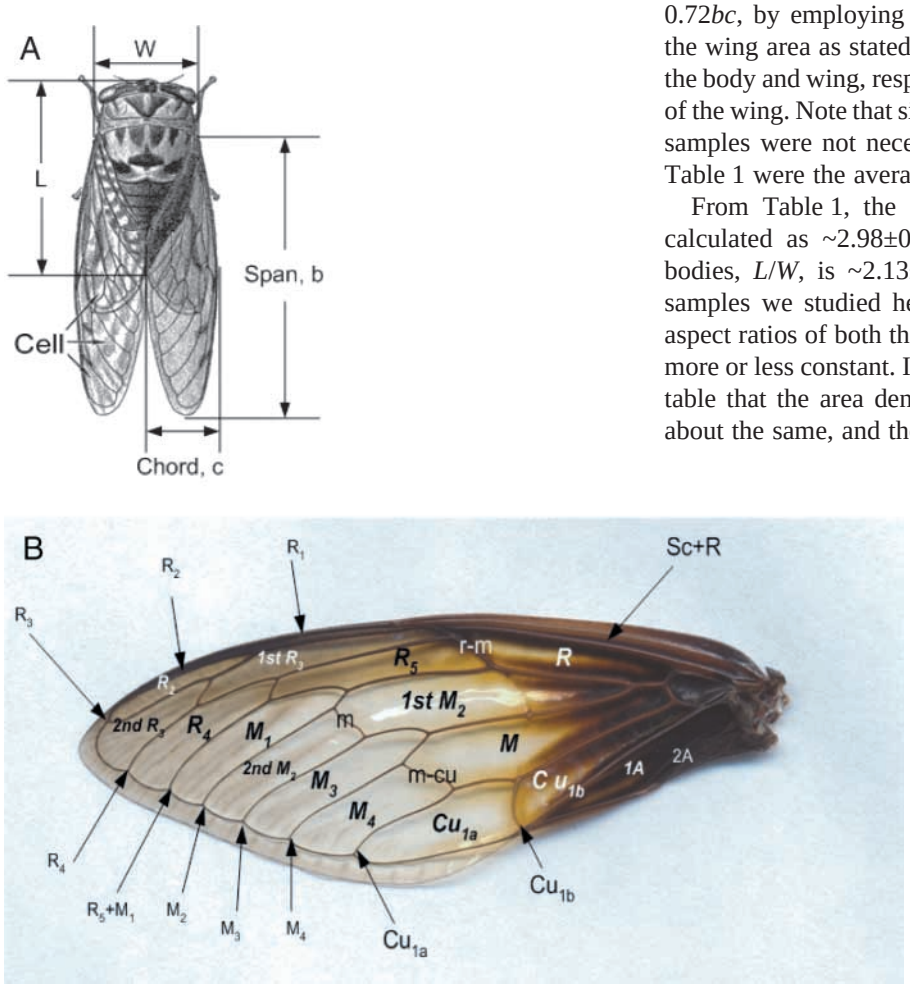

Fig. 2. (A) Scanning image of a cicada showing some structural and morphological definitions (modified from Borror and White, 1970). L, body length; W, body width; b, wing span; c, wing chord. (B) Scanning image of the forewing of cicada showing the longitudinal veins, cross veins and cells of the wing designated by the Comstock–Needham system.

Table 1. *Morphological data of the forewing and the body of cicada*

Samples	1	2	3	4	5	Mean ± S.D.
L (mm)	33.41	37.94	43.13	37.63	35.11	37.44±3.30
W (mm)	15.48	17.85	20.14	17.50	16.19	17.43±1.60
b (mm)	44.57	50.79	52.13	50.02	48.51	49.20±2.60
c (mm)	14.39	17.15	17.63	16.90	16.19	16.45±1.13
A (mm^2)	461.78	627.15	661.72	608.64	565.47	584.95±68.97
M_b (g)	1.22	1.72	1.84	1.68	1.55	1.60±0.21
M_w (mg)	12.9	18.0	19.2	17.3	16.1	16.70±2.15
λ (mg mm^{-2})	0.0279	0.0287	0.0290	0.0284	0.0285	0.0285±0.0004

Abbreviations: A, area of wing; b, wing span; c, wing chord; L, body length; M_b, body mass; M_w, wing mass; W, body width; λ, area density of wing.

The cross-sectional diameters of the veins along the venation on the cicada wings were very asymmetric, for example the maximum and the minimum diameters of the veins of the forewings were separately found on the veins Sc and M_4, respectively, as shown in Fig. 2B, and were measured as approximately 256.3 μm and 50.8 μm, respectively. We measured the vein diameters of the forewings from the five cicada samples and obtained the mean ± S.D. of the veins of the wings (133.6±68.9 μm). In particular, the mean diameter of the leading edges of the forewings was ~255.7 μm.

In addition, the veins of the leading edge, i.e. Sc+R, as shown in Fig. 2B, were cut from the forewings. Since these veins were hollow in the center and were similar to two pipes parallel to each other along the direction of the leading edge of the wings, both pipes were carved and the mean wall thickness of the pipes was measured as ~37.8 μm. Thus, the mean diameter of each hole on the cross sections of the leading edges was approximately 180 μm.

The thickness for each of the cells of the forewing was measured and is presented in Table 2. In addition, the mean thickness of the membrane that was near the edge of the wing and outside the cells (Fig. 2B) was measured as ~8.5 μm. This clearly shows that the thickness of the cell membrane on the wings was not uniform. The mean ± S.D. of the thickness of the cells was approximately computed to be 12.2±1.3 μm. Note that the mean ± S.D. of the thickness of the cells in Table 2 does not contain that of the membrane near the edge and outside the cells. Based on the mean thickness of membrane, the mean density of the forewing, including the membrane and the vein, was estimated to be approximately 2.3 g cm^{-3}.

Mechanical tests

The measurements of the line profile of the membrane surface of the wing cells indicate that the mean asperity height (the height from the mean surface to the real surface) was ~18 nm, which is sufficiently flat for performing nanoindentation.

Fig. 3A shows a typical plot of nanoindentation load *versus* displacement data for a cell membrane. Note that no significant sink-in or pile-up was observed along the sides of the triangular indentation in the image obtained using a topographic scanning electron microscope, as shown in Fig. 3B. This illustrates that the difference between the hardness of the membrane and that of the substrate was very small. In fact, the substrate was found to be a little harder than the membrane from the indentation data below. Saha and Nix (2002) pointed out that the effect of substrate hardness on the film hardness was negligible in the case of soft film on hard substrate.

In order to characterize the effects of the substrate on the membrane hardness and Young's modulus, the parameter P/S^2 was analyzed as a function of the indentation depth relative to the membrane's thickness (Joslin and Oliver, 1990). For

Table 2. *The mean thickness (*t*), Young's modulus (*E*) and hardness (*H*) of the cells*

Cell	R	R_2	1st R_3	2nd R_3	R_4	R_5	M_1	1st M_2	2nd M_2	M_3	M	M_4	Cu_{1a}	Cu_{1b}	1A
t (μm)	15.2 ± 0.92	12.3 ± 0.76	14.5 ± 0.97	10.2 ± 0.55	10.8 ± 0.87	13.8 ± 0.47	10.8 ± 0.34	13.4 ± 0.76	11.5 ± 0.44	12.8 ± 0.53	14.6 ± 0.88	12.5 ± 0.34	13.1 ± 0.54	15.3 ± 0.97	15.2 ± 0.90
E (GPa)	3.72 ± 0.33	3.85 ± 0.09	3.83 ± 0.07	3.78 ± 0.12	3.75 ± 0.41	3.59 ± 0.30	3.66 ± 0.17	3.56 ± 0.02	3.63 ± 0.15	3.57 ± 0.17	3.79 ± 0.07	3.55 ± 0.14	3.56 ± 0.15	3.82 ± 0.08	3.77 ± 0.15
H (GPa)	0.21 ± 0.072	0.23 ± 0.019	0.23 ± 0.047	0.22 ± 0.011	0.19 ± 0.004	0.17 ± 0.017	0.18 ± 0.006	0.17 ± 0.006	0.18 ± 0.040	0.17 ± 0.002	0.21 ± 0.018	0.18 ± 0.034	0.17 ± 0.008	0.23 ± 0.007	0.19 ± 0.173

Values are means ± S.D.

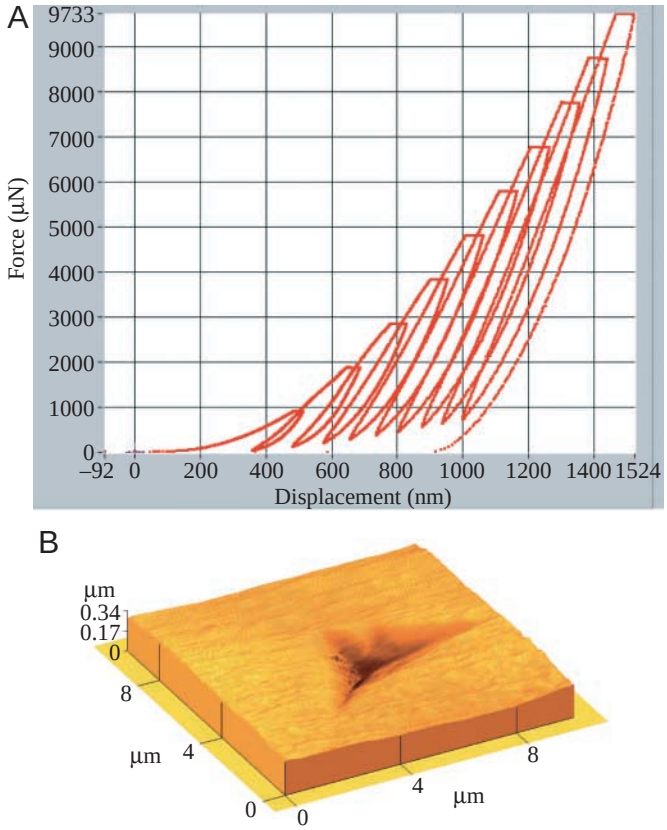

Fig. 3. (A) Plot of applied load *versus* penetration depth. (B) Atomic force microscope image of nanoindention showing the indented shape made by a triangular pyramid Berkovich indenter.

homogeneous materials, P/S^2 should be constant with respect to the indentation depth. Fig. 4 displays the variation of P/S^2 with indentation depth of some trials. It can be seen that the parameter P/S^2 remained constant when the depth was less than 600 nm, beyond which it increased until 1600 nm. This proved that the effects of the substrate were insignificant unless the

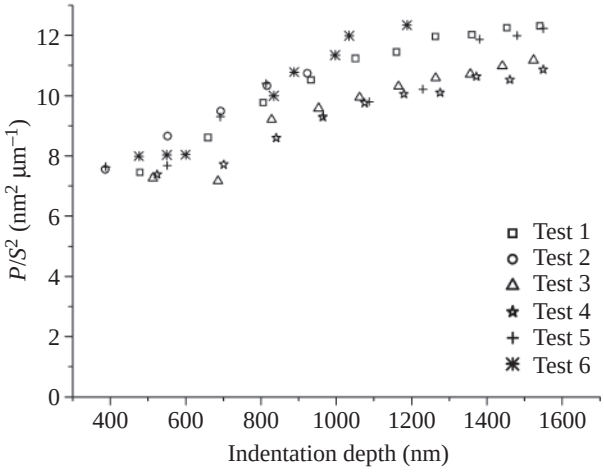

Fig. 4. Plot of P/S^2 as a function of indentation depth for the membrane tested.

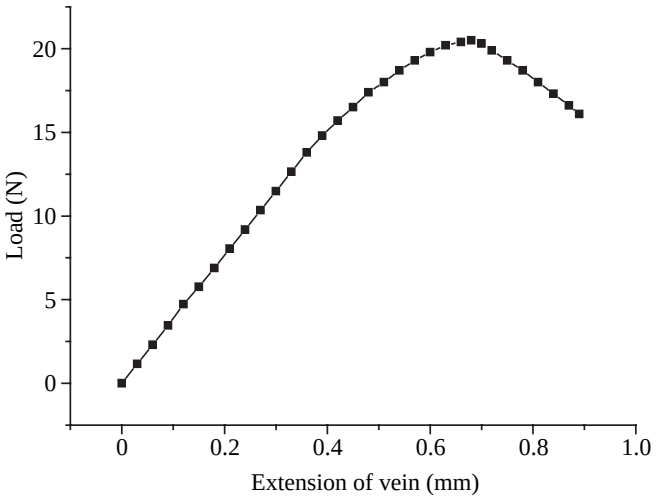

Fig. 5. Curve of load *versus* extension for a vein tested.

indentation depth was greater than 5% of the membrane thickness, which was ~12.2 μm. It is important to note that only the data collected from indentation depths below 600 nm were used to calculate the material properties.

From the above equations and experimental data, the Young's modulus and hardness of the membrane were calculated as ~3.7 GPa and 0.2 GPa, respectively. Table 2 presents such values for each cell membrane.

The mechanical properties of the veins were firstly tested. A typical load-displacement curve for the vein from the leading edge of a forewing is shown in Fig. 5. The elastic force and elastic deformation were measured to be F_e=13.8 N and Δl_e=0.36 mm, respectively. The force and deformation corresponding to the strength of the material were F_{th}=20.5 N and Δl_{th}=0.68 mm, respectively. Since there were two holes in the vein at a leading edge, Sc+R (Fig. 2B), the original cross-sectional area of the vein, A_0, should exclude that of the holes; therefore, A_0=390.8×10^{-3} mm^2. As a result, the Young's

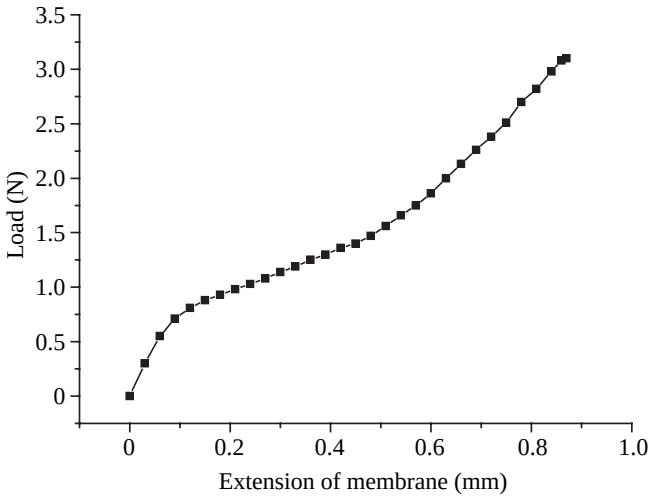

Fig. 6. Curve of load *versus* extension for a cell membrane tested.

modulus, E, and the strength, σ_{th}, of the vein were approximately 1.9 GPa and 52 MPa, respectively.

Secondly, as a verification of the above nanoindentation test data, tensile testing of the membranes was carried out to determine the Young's modulus and strength for comparison. Fig. 6 shows a typical tensile curve of the membrane cut-off from the cell M_3 of the wing (Fig. 2B). From this figure, the elastic force and deformation were determined to be F_e=0.58 N and Δl_e=0.06 mm, respectively. Hence, the Young's modulus of the membrane was calculated to be ~3.87 GPa. Moreover, the yield stress of the membrane was determined to be ~29 MPa.

Discussion

In terms of the structures of the forewing of cicada, the vein diameters of the wing were found to be nonuniform; in general, the further the position of the vein from the wing base, the smaller was its diameter. Similar to the distribution of the veins on the wing, the further the location of the cell from the base of the wing, the thinner was the cell membrane. However, the difference between the thickness of the membranes of the cells was quite small and can be approximately considered to be uniform.

For the material properties of the wings, two methods were employed to measure the Young's modulus of the membrane. The Young's moduli obtained by the two methods were in good agreement with each other. It was found that the Young's modulus of the cicada (3.7 GPa) was lower than that of locust membrane (5 GPa), α-keratin (4 GPa), β-keratin (8–10 GPa) and lepidopteran silk (10 GPa) (Smith et al., 2000) but was much higher than some amorphous protein polymers, e.g. resilin (1.2 MPa; Gosline, 1980) and abductin (4 MPa; Alexander, 1966). In fact, it was not only the Young's modulus of the cicada that was very close to that of most synthetic amorphous protein polymers (~4 GPa), as the typical load-displacement curve (Fig. 6) for the membrane of the former was also similar to that of the latter. Thus, the said material is probably a convenient choice for biomimetic design of the aerofoil of small vehicles. However, more understanding of the wing's structures and the flight mechanism is needed in order to synthesize the biomechanical and performance studies.

From the results given above, it can be seen that the strength of the vein was greater than the yield stress of the membrane, whereas the stiffness of the membrane was greater than that of the vein. From the viewpoint of mechanics, the results should be deemed reasonable. The venation of the wing can be regarded as the framework of the wing. If the strength of the framework is too low or the stiffness of the framework is too high, the wing can be broken easily and the flight capability would be affected. The membrane of the wing is similar to a sail. If the stiffness and yield stress of the sail are too low, the flight performance would be deflected easily. It is an indication that in future design of the aerofoil of micro air vehicles, biomimetic design that involves both the aerofoil structures and the mechanical properties of the aerofoil materials selected will be employed. The results of this study should be viewed as preliminary results, which are subject to further testing incorporating flight performance. However, it is worthwhile noting that this study introduces an approach for direct measurement of the biomechanical properties of the wings of insects.

The authors are grateful to the referees for their critical reviews. This work was supported by the National Natural Science Foundations of China (Grant 10372102) and William Mong Research Fund (donated to the University of Hong Kong).

References

Alexander, R. McN. (1966). Rubber-like properties of the inner hinge-ligament of Pectinidae. *J. Exp. Biol.* **44**, 119-130.

Banerjee, S. (1988). The functional significance of wing architecture in acridid Orthoptera. *J. Zool. Lond.* **215**, 249-267.

Birch, J. M. and Dickinson, M. H. (2001). Spanwise flow and the attachment of the leading-edge vortex on insect wings. *Nature* **412**, 729-733.

Borror, D. J. and White, R. E. (1970). *Field Guide to Insects: America North of Mexico*. Boston: Houghton Mifflin.

Borror, D. J., Triplehorn, C. A. and Johnson, N. F. (1989). *An Introduction to the Study of Insects*. Sixth edition. New York: Saunders College Publishing.

Chapman, R. F. (1998). *The Insects: Structure and Function*. 4th edition. Cambridge: Cambridge University Press.

Dickinson, M. H., Lehmann, F.-O. and Sane, S. P. (1999). Wing rotation and the aerodynamic basis of insect flight. *Science* **284**, 1954-1960.

Ellington, C. P., Van Den Berg, C., Willmott, A. P. and Thomas, A. L. R. (1996). Leading-edge vortices in insect flight. *Nature* **284**, 626-630.

Fearing, R. S., Chiang, K. H., Dickinson, M. H., Pick, D. L., Sitti, M. and Yan, J. (2000). Wing transmission of a micromechanical flying insect. In *Proceedings of the 2000, IEEE. International Conference on Robotics and Automation, San Francisco, CA* (ed. D. L. Alessandro), pp. 1509-1516. New Jersey: Wiley & Sons.

Fonseca, P. J. and Revez, M. A. (2002). Song discrimination by male cicadas Cicada Barbara lusitanica (Homoptera, Cicadidae). *J. Exp. Biol.* **205**, 1285-1292.

Fonseca, P. J., Münch, D. and Hennig, R. M. (2000). How cicadas interpret acoustic signals. *Nature* **405**, 297-298.

Gosline, J. M. (1980). The elastic properties of rubber-like proteins and highly extensile tissues. In *The Mechanical Properties of Biological Materials* (ed. J. F. V. Vincent and J. D. Currey), pp. 331-358. Cambridge: Cambridge University Press.

Herbert, R., Young, P. G., Smith, C. W., Wootton, R. J. and Evans, K. E. (2000). The hind wing of the desert locust (*Schistocerca gregaria* Forskål). III. A Finite element analysis of a deployable structure. *J. Exp. Biol.* **203**, 2945-2955.

Ho, S., Nassaf, H., Pornsin-Sirirak, N., Tai, Y.-C. and Ho, C.-M. (2002). Flight dynamics of small vehicles. In *Proceedings of the International Council of the Aeronautical Sciences (ICAS)* (ed. I. Grant), pp. 551.1-551.10. Toronto, Canada: ICAS.

Jensen, M. and Weis-Fogh, T. (1962). Biology and physics of locust flight. V. Strength and elasticity of locust cuticle. *Phil. Trans. R. Soc. Lond. B* **245**, 137-169.

Joslin, D. L. and Oliver, W. C. (1990). A new method for analyzing data from continuous depth-sensing microindentation tests. *J. Mater. Res.* **5**, 123-126.

Maxworthy, T. (1979). Experiments on the Weis-Fogh mechanism of lift generation by insects in hovering flight. Part 1. Dynamics of the "fling". *J. Fluid Mech.* **93**, 47-63.

Oliver, W. C. and Pharr, G. M. (1992). An improved technique for determining hardness and elastic-modulus using load and displacement sensing indentation experiments. *J. Mater. Res.* **7**, 1564-1583.

Saha, R. and Nix W. D. (2002). Effects of the substrate on the determination of thin film mechanical properties by nanoindentation. *Acta Materialia* **50**, 23-38.

Smith, C. W., Herbert, R., Wootton, R. J. and Evans, K. E. (2000). The hind wing of the desert locust (*Schistocerca gregaria* Forskål). II.

Mechanical properties and functioning of the membrane. *J. Exp. Biol.* **203**, 2933-2943.

Van Den Berg, C. and Ellington, C. P. (1997). The three-dimensional leading-edge vortex of the hovering model hawkmoth. *Phil. Trans. R. Soc. Lond. B* **353**, 329-340.

Weis-Fogh, T. and Jensen, M. (1956). Biology and physics of locust flight. I. Basic principles in insect flight. A critical review. *Phil. Trans. R. Soc. Lond. B* **239**, 415-458.

Wolf, B. and Richter A. (2003). The concept of differential hardness in depth sensing indentation. *New J. Phys.* **5**, 15.1-15.17.

Wootton, J. R. (1992). Functional morphology of insect wings. *Annu. Rev. Entomol.* **37**, 113-140.

Wootton, R. J., Evans, K. E., Herbert, R. and Smith, C. W. (2000). The hind wing of the desert locust (*Schistocerca gregaria* Forskål). I. Functional morphology and mode of operation. *J. Exp. Biol.* **203**, 2921-2931.